AD-A059 858 PENNSYLVANIA STATE UNIV UNIVERSITY PARK APPLIED RESE--ETC F/G 20/1
ON THE RADIATED NOISE DUE TO BOUNDARY-LAYER TRANSITION.(U)
JUL 78 G C LAUCHLE N00017-73-C-1418

UNCLASSIFIED ARL/PSU/TM-78-204 NL

1 OF 1
AD A059858

END
DATE FILMED
12-78
DDC

(12) LEVEL II

NW

(6) ON THE RADIATED NOISE DUE TO BOUNDARY-LAYER TRANSITION

(10) G. C./Lauchle

(14) ARL/PSU/TM-78-204

(9) Technical Memorandum
File No. TM 78-204
(11) 28 July [illegible], 1978
Contract No. N00017-73-C-1418

(15) Copy No. 48

(12) 53 p.

The Pennsylvania State University
Institute for Science and Engineering
APPLIED RESEARCH LABORATORY
Post Office Box 30
State College, Pa. 16801

NAVY DEPARTMENT

NAVAL SEA SYSTEMS COMMAND

Approved for Public Release
Distribution Unlimited

UNCLASSIFIED

SECURITY CLASSIFICATION OF THIS PAGE *(When Data Entered)*

REPORT DOCUMENTATION PAGE		READ INSTRUCTIONS BEFORE COMPLETING FORM
1. REPORT NUMBER TM 78-204	2. GOVT ACCESSION NO.	3. RECIPIENT'S CATALOG NUMBER
4. TITLE *(and Subtitle)* ON THE RADIATED NOISE DUE TO BOUNDARY-LAYER TRANSITION (U)		5. TYPE OF REPORT & PERIOD COVERED Technical Memorandum 6. PERFORMING ORG. REPORT NUMBER
7. AUTHOR*(s)* G. C. Lauchle		8. CONTRACT OR GRANT NUMBER*(s)* N00017-73-C-1418
9. PERFORMING ORGANIZATION NAME AND ADDRESS Applied Research Laboratory P.O. Box 30 State College, PA 16801		10. PROGRAM ELEMENT, PROJECT, TASK AREA & WORK UNIT NUMBERS
11. CONTROLLING OFFICE NAME AND ADDRESS Naval Sea Systems Command Washington, DC 20362		12. REPORT DATE July 28, 1978 13. NUMBER OF PAGES 45
14. MONITORING AGENCY NAME & ADDRESS*(if different from Controlling Office)*		15. SECURITY CLASS. *(of this report)* UNCLASSIFIED 15a. DECLASSIFICATION/DOWNGRADING SCHEDULE

16. DISTRIBUTION STATEMENT *(of this Report)*

Approved for Public Release. Distribution Unlimited.
Per NAVSEA - Sept. 27, 1978.

17. DISTRIBUTION STATEMENT *(of the abstract entered in Block 20, if different from Report)*

18. SUPPLEMENTARY NOTES

19. KEY WORDS *(Continue on reverse side if necessary and identify by block number)*

laminar flow
boundary layer
noise
transition
acoustic pressure

20. ABSTRACT *(Continue on reverse side if necessary and identify by block number)*

(U) A theory is presented for the noise radiated by incompressible boundary-layer transition that occurs on an infinite, rigid flat plate. It is hypothesized that it is the intermittency of the boundary-layer flow within the transition zone that is dominant in noise production. Using Lighthill's analogy, it is shown that dipole, quadrupole, and octupole sources are generated. Under the assumption of low Mach number flow, the power spectral density per unit spanwise width of transition

DD FORM 1 JAN 73 1473 EDITION OF 1 NOV 65 IS OBSOLETE

UNCLASSIFIED

SECURITY CLASSIFICATION OF THIS PAGE *(When Data Entered)*

for the radiated acoustic pressure is derived for the dipole contribution (which is acoustically more efficient than the other sources by a factor inversely proportional to the Mach number squared). The spectral shape corresponds to one obtained by passing white noise through a realizable bandpass filter. The low-frequency cutoff scales with the burst frequency associated with turbulent spot formation, and the high-frequency cutoff scales inversely with the time required for the wall shear stress to change from a laminar value to a turbulent value at a given point of local laminar flow breakdown. As one example, the theory is used to predict the noise radiated by an under-water buoyant body for which there are experimental data. The comparison is found to be very good at low frequencies, and reasonably good at the high-frequency end of the spectrum. However, if the acoustic energy generated by the fully-developed turbulent flow over the body is added to the energy generated by the transition zone, then the entire predicted spectrum agrees to within 3 dB of the one measured.

Subject: On the Radiated Noise due to Boundary-Layer Transition

References: See page 34

Abstract: A theory is presented for the noise radiated by incompressible boundary-layer transition that occurs on an infinite, rigid flat plate. It is hypothesized that it is the intermittency of the boundary-layer flow within the transition zone that is dominant in noise production. Using Lighthill's analogy, it is shown that dipole, quadrupole, and octupole sources are generated. Under the assumption of low Mach number flow, the power spectral density per unit spanwise width of transition for the radiated acoustic pressure is derived for the dipole contribution (which is acoustically more efficient than the other sources by a factor inversely proportional to the Mach number squared). The spectral shape corresponds to one obtained by passing white noise through a realizable bandpass filter. The low-frequency cutoff scales with the burst frequency associated with turbulent spot formation, and the high-frequency cutoff scales inversely with the time required for the wall shear stress to change from a laminar value to a turbulent value at a given point of local laminar flow breakdown. As one example, the theory is used to predict the noise radiated by an underwater buoyant body for which there are experimental data. The comparison is found to be very good at low frequencies, and reasonably good at the high-frequency end of the spectrum. However, if the acoustic energy generated by the fully-developed turbulent flow over the body is added to the energy generated by the transition zone, then the entire predicted spectrum agrees to within 3 dB of the one measured.

Acknowledgements

The author acknowledges Dr.'s D. G. Crighton and J. L. Lumley for various helpful discussions related to this analysis. The sponsorship of the U.S. Naval Sea System Command, Code 0351 is also gratefully appreciated.

TABLE OF CONTENTS

LIST OF FIGURES

July 28, 1978
GCL:jrp

NOMENCLATURE

A	Defined through eq. (39)
a	a constant, 4.185
B	Defined through eq. (39)
b	a constant, 2.544
c	velocity of sound in the acoustic medium
D	diameter of body
F	frequency integral given by eq. (50)
G	power spectrum for the acoustic pressure
g	Emmons' source-rate density function
I	the ideal indicator function
$\tilde{I}$	a more realistic indicator function
$\|J\|^2$	frequency depression factor
L_3	spanwise integral length scale associated with bursts
M	Mach number
N	expected number of turbulence bursts per unit time
p	acoustic pressure (also p')
R	time correlation function of I at given x_1
R_1	standard deviation of I at given x_1
R_3	spanwise spatial correlation function of I
$\tilde{R}, \tilde{R}_1, \tilde{R}_3$	same as R, R_1, R_3, but for $\dot{I}$
Re_t	transition Reynolds number
Re_u	unit Reynolds number
Re_{x_1}	Reynolds number based on x_1
$Re_{\Delta x}$	Reynolds number based on Δx
Re_Θ	Reynolds number based on Θ
r	observation point coordinate

S	surface area of hydro/acoustic source region
s	Laplace transform variable
T	sample time
t	time
t_i	rise time for wall shear stress to change state
T_{ij}	Lighthill's stress tensor
u_c	convection velocity of turbulence bursts
u_i	fluid velocities (i=1,2,3)
u_L	laminar boundary layer velocity profile
u_ℓ	leading-edge velocity of turbulence burst
u_0	free-stream velocity
u_T	turbulent boundary layer velocity profile
u_t	trailing-edge velocity of turbulence burst
u_*	friction velocity
V	volume of hydro/acoustic source region
V'	volume of hydro-acoustic image source region
V_0	amplitude of $\tilde{\dot{I}}$
x_i	Cartesian coordinates (i=1,2,3)
$\bar{x}_1$	non-dimensional form of x_1
x_0	the value of x_1 at the beginning of intermittent flow
Δx	streamwise extent of intermittent flow
α	one-half the apex angle of wedge formed by the locus of a turbulence burst as it convects downstream
γ	the intermittency factor
Δ	the retarded time delay $\tau - \xi_1/u_c$
δ_{ij}	Kronecker delta function
ε	a small quantity
η_i, ξ_i, ϕ_i	variables of integration
Θ	viscous sub-layer thickness

θ aspect angle

κ free-stream convection wavenumber

Λ defined by eq. (29)

ν kinematic viscosity

ρ fluid mass density

ρ' fluctuating mass density

σ the difference $\tau_T - \tau_L$

σ_{ij} viscous stress tensor

σ^* defined by eq. (45)

τ time delay

τ_0 fluctuating wall shear stress, $\sigma_{12}|_{x_2=0}$

τ_L laminar boundary-layer value of wall shear stress

τ_T turbulent boundary-layer value of wall shear stress

ω radian frequency

Special notation

$\dot{(\text{-})}$ implies time derivative

<---> implies expectation value

I. INTRODUCTION

By contrast with the number of papers devoted to the investigation of noise radiated by a region of fully-developed turbulence, only a few have addressed the sound field generated by the laminar-to-turbulent transition zone [1 - 4]. Ffowcs - Williams [1] discusses the transition zone noise in terms of the initial formation of turbulence spots. The elegant analysis of a three-dimensional disturbance growing in accordance with the equations of linear stability theory by Brooke Benjamin [5] was incorporated into Lighthill's theory [6] for the radiating component of flow noise. A quadrupole source was assumed and it was thus shown that sound radiation would occur essentially only when the wall was of pressure release type. For an assumed rigid surface the imaging effect transforms the quadrupoles into much less efficient octupole radiators. Furthermore, even for the soft surface, the analysis shows that it is only at the very beginning of spot formation where sound is generated. Farther downstream the spot grows exponentially, but the sound pressure is found to decrease exponentially with time. Of course it could be argued that the linear stability model breaks down as a spot develops which may account for this conclusion. Ffowcs - Williams points out that the theory may be applicable only if sound is truly generated in the early stages of instability, but late enough such that the asymptotic theory of Brooke Benjamin is established, while at the same time the spot amplitude is still small.

Dolgova [4] considered the planar flow over a rigid surface and analyzed the sound radiated by only the Tollmien - Schlichting wave growth.

As in linear stability models he let a pressure wave grow exponentially in the direction of flow, and then applied Fourier and Hankel transforms to obtain an expression for the sound pressure and directivity function. At low frequencies the pattern is dipole while at higher frequencies the main lobe tilts to the downstream direction, gets sharper, and develops several side lobes. The resulting expression for the sound pressure, however, shows no Mach number dependence.

Natural transition is characterized by essentially three distinct, flow regimes. In the early stages of instability, the laminar boundary layer becomes disturbed in a linear, wavelike manner. It is here where the theory of Dolgova [4] is applicable. Farther downstream, these linear disturbances become more non-linear and three dimensional. The analysis of Ref. [1] appears to be applicable in this regime, but breaks down rapidly as turbulent bursts begin to form. Within this third flow regime, where the boundary layer intermittently alternates between laminar and turbulent, is where no fundamental flow noise theory has yet been developed. We hypothesize that this region of intermittent boundary-layer flow may give rise to intense sound radiation [2,3]. We know from elementary boundary-layer theory that the mean velocity gradients and profiles are quite different between laminar and turbulent flow over surfaces. In intermittent flow, we would expect that the wall shear stress (and other viscous stresses) and the mean boundary layer velocities, both parallel and normal to the surface, undergo gross fluctuations in time. According to Lighthill's analogy [6], fluctuating velocities give rise to quadrupole noise sources, while fluctuating wall shear stresses give rise to dipole sources [7]. At very low Mach numbers, M, this latter source would be

expected to dominate the noise field. This is deduced from the fact that the acoustic efficiency of dipole sources is of the order M^3, while that of quadrupole sources is of order M^5, viz., Ross [8]. From noise measurements the author made [3] on an axisymmetric body with flush-mounted hydrophones placed in and around the transition zone, the variation is spectral level with velocity seemed to imply a dipole - type of source.

In this paper we will approach analytically the problem of noise generated by intermittent boundary-layer flow as it occurs in natural transition on a flat plate. We will assume the plate to be infinite in extent and to be acoustically rigid. We will further assume incompressible hydrodynamics describe the transitional process. Our goal is to derive an expression for the radiated noise spectrum. This spectrum, because of our infinite extent assumption, will be derived in terms of the sound pressure radiated per unit spanwise width of transition. Under the assumptions that the acoustic wavelength is large, and that the boundary layer is thin relative to a given local radius of curvature, this theory should have direct application to axisymmetric bodies and hydrofoils. One would simply multiply the predicted spectrum by the circumference of the body at the transition point (or the span of the hydrofoil at this point) to get the overall acoustic spectrum.

As examples of the analysis, we will compute the radiated noise spectra corresponding to the experimental conditions of Ref.'s [2] and [3], compare them with the experimental data, and discuss the correlation in terms of transitional flow noise and fully-developed turbulent flow noise contributions. The theory presented here, for the noise radiated by boundary-layer transition, suggests the critical hydrodynamic parameters that govern this noise.

II. ANALYSIS

Consider the uniform flow over a flat plate. If a laminar boundary layer begins to form at the origin of our Cartesian coordinate system, and if the flow direction is in the x_1-direction, then the flow will ultimately become non-linearly unstable at the downstream line $x_1=x_0$ (see Fig. 1). There is then a short distance, Δx, over which turbulent "bursts" occur. Along $x_1 = x_0 + \Delta x$, the flow becomes fully turbulent while for $x_1 < x_0$, the flow is assumed completely laminar. In the analysis to follow, we will treat $\Delta x dx_3 dx_2$ as our source volume.

The equation that describes the sound radiation from fluid-dynamic sources is the well-known Lighthill equation [6]:

$$\frac{\partial^2 \rho'}{\partial t^2} - c^2 \frac{\partial^2 \rho'}{\partial x_i \partial x_j} = \frac{\partial^2 T_{ij}}{\partial x_i \partial x_j} , \qquad (1)$$

where ρ' is the fluctuating density, t is time, c is the sound velocity in the medium surrounding the source region, and T_{ij} is Lighthill's stress tensor given by:

$$T_{ij} = \rho u_i u_j - \sigma_{ij} + (p'-\rho' c^2)\delta_{ij}, \qquad (2)$$

where ρ is the mean density.

Composing this tensor is $\rho u_i u_j$, the fluctuating Reynolds stress tensor; σ_{ij}, the fluctuating viscous shear stress tensor; and $(p'-\rho' c^2)$, a term that relates to heat conduction or non-linearity. For hydrodynamic flows, this last term is zero which means that the fluctuating density is related to the fluctuating pressure by

$$p' = \rho' c^2. \qquad (3)$$

From this point on, we will drop the prime from the fluctuating quantities, and solve eq. (1) for the acoustic pressure through use of eq. (3).

A. T_{ij} for Boundary-Layer Transition

Within the region $x_0 \leq x_1 \leq x_0 + \Delta x$, the flow intermittently changes from laminar to turbulent regimes. A typical turbulence burst is shown schematically in Fig. 2. A burst will grow as it convects downstream at a mean convection velocity, u_c. The locus of a typical burst forms a wedge of apex angle 2α. Emmons [9] first observed α to be on the order of 9.6° for flat plate flows. This was reconfirmed later by Schubauer and Klebanoff [10], although it should be pointed out that Farabee, et.al. [11] found propagation angles significantly greater than this.

In reference to the elevation view of Fig. 2, we see that at a given point on the x_1-axis, the mean velocity profile and the wall shear stress will undergo gross fluctuations in time as bursts are swept by. We will assume that these fluctuations are much larger than the velocity and shear stress fluctuations that occur within a burst itself or within the fully-developed turbulent boundary layer that occurs at $x_1 > x_0 + \Delta x$. For example, the wall shear stress under a turbulent boundary layer can be calculated from [12]:

$$\tau_T(x_1) = 0.0288\rho u_0^2 (u_0 x_1/\nu)^{-1/5}, \qquad (4)$$

while at some other instant of time, when the boundary layer is laminar at x_1:

$$\tau_L(x_1) = 0.332\rho\nu u_0 (\nu x_1/u_0)^{-1/2}, \qquad (5)$$

where ν is the kinematic viscosity. Thus, as the flow regime alternates between laminar and turbulent, we might expect fluctuations in the

wall shear stress on the order of

$$\frac{\sigma(x_1)}{\tau_T(x_1)} \equiv \frac{\tau_T - \tau_L}{\tau_T} = 1 - 11.53(Re_{x_1})^{-3/10} \quad , \qquad (6)$$

where $Re_{x_1} = u_0 x_1 / \nu$ is the local value of length Reynolds number. Typically, $Re_{x_0} \simeq 3 \times 10^6$, so $\sigma(x_0) \simeq 0.9\tau_T(x_0)$. On the other hand, under a fully-developed turbulent boundary layer, the magnitude of the fluctuating wall shear stress relative to τ_T (as deduced from the measurements of Lu and Willmarth [13])is of order 0.1. Thus, our assumption regarding the magnitude of the wall shear stress fluctuations during bursting flow seems justified. Similar arguments can be set down for the fluctuations in mean velocity.

Consequently, eq. (2) for T_{ij} may be written

$$T_{ij} \approx \rho u_i u_j - \tau_0(x_i,t) \quad , \qquad (7)$$

where

$$\tau_0(x_i,t) = \sigma_{12}|_{x_2 = 0} >> \sigma_{ij}(ij \neq 12) \qquad (8)$$

which is the fluctuating wall shear stress due to the creation and convection of turbulence bursts. If we further assume (because of the slow rate at which a burst spreads laterally) that the mean velocity fluctuation in the x_3-direction is small compared to u_1 and u_2, then T_{ij} will have only three dominant components in addition to $\tau_0(x_1,t)$.

We have not yet been explicit regarding the time dependence of τ_0, u_1, and u_2. It will prove expedient to first solve eq. (1) subject to our assumed form of T_{ij} and the appropriate acoustic boundary conditions.

B. Formal Solution

The solution to eq. (1) for flow over arbitrary surfaces was first constructed by Curle [14]. Powell [15] showed that when the surface is rigid and planar, one could consider a new extended flow field obtained by reflection of the original one in the plane $x_2 = 0$, as illustrated in Fig. 3(a). Using Powell's result, we find

$$p(\mathbf{r},t) = c^2\rho'(\mathbf{r},t) = \frac{\rho}{4\pi}\,\frac{\partial^2}{\partial x_i \partial x_j}\iiint_{V+V'}\frac{u_i u_j}{r}\,dV - \frac{1}{2\pi}\,\frac{\partial}{\partial x_1}\iint_S \frac{\tau_0}{r}\,dS, \qquad (9)$$

where the integrands are functions of the retarded time variable (t-r/c) and primes refer to the image-flow side of the plane. The radial coordinate defining the point of observation is

$$r = |\bar{x} - \bar{\eta}|, \qquad (10)$$

where $\bar{\eta}$ denotes the dummy variable of integration. By making the far-field assumption, we can let $r \simeq r' \simeq |\bar{x}|$, and then noting that

$$\frac{\partial|\bar{x}|}{\partial x_i} = \frac{\partial\{x_1+x_2+x_3\}^{1/2}}{\partial x_i} = \frac{x_i}{|\bar{x}|} \qquad (11)$$

we let

$$\frac{\partial}{\partial x_i} = \frac{\partial|\bar{x}|}{\partial x_i}\,\frac{\partial t'}{\partial|\bar{x}|}\,\frac{\partial t}{\partial t'}\,\frac{\partial}{\partial t},$$

where $t' \equiv t - |\bar{x}|/c$. From this we obtain the identities:

$$\frac{\partial}{\partial x_i} = -\frac{1}{c}\,\frac{x_i}{r}\,\frac{\partial}{\partial t} \qquad (12)$$

and

$$\frac{\partial^2}{\partial x_i \partial x_j} = \frac{1}{c^2} \frac{x_i x_j}{r^2} \frac{\partial^2}{\partial t^2} \quad . \tag{13}$$

Equation (9) may now be rewritten in the form:

$$4\pi r c^2 p(r,t)/\rho = \left(\frac{x_1}{r}\right)^2 \frac{\partial^2}{\partial t^2} \iiint_V u_1^2 dV + 2\frac{x_1 x_2}{r^2} \frac{\partial^2}{\partial t^2} \iiint_V u_1 u_2 dV$$

$$+ \left(\frac{x_2}{r}\right)^2 \frac{\partial^2}{\partial t^2} \iiint_V u_2^2 dV + \left(\frac{x_1}{r}\right)^2 \frac{\partial^2}{\partial t^2} \iiint_{V'} (u_1')^2 dV' + 2\frac{x_1 x_2}{r^2} \frac{\partial^2}{\partial t^2} \iiint_{V'} u_1' u_2' dV'$$

$$+ \left(\frac{x_2}{r}\right)^2 \frac{\partial^2}{\partial t^2} \iiint_{V'} (u_2')^2 dV' + 2\frac{c}{\rho} \left(\frac{x_1}{r}\right) \frac{\partial}{\partial t} \iiint_S \tau_0 dS. \tag{14}$$

Each of the terms composing eq. (14) represent a hydrodynamically - generated acoustic source. The direction cosine preceeding each integral tells us the order and orientation of each of these sources. We see that the first and fourth terms have a $\cos^2\theta$ directivity characteristic (see Fig. 1 for definition of θ), indicating that they are longitudinal quadrupoles with axes parallel to the surface. These two sources, one being in the image flow combine constructively to form a single longitudinal quadrupole of twice the strength of one alone. The second and fifth terms represent lateral quadrupoles because of the cross-term products and directivity function $\sin\theta \cos\theta$. However, when combining a lateral quadrupole with its image, a less efficient octupole results. We can safely neglect those source terms involving $u_1 u_2$ and $u_1' u_2'$ under our low Mach number assumption. The third and sixth terms also represent longitudinal quadrupoles, but because $(x_2/r)^2 = \sin^2\theta$ their axes are

perpendicular to the surface; when combined, complete cancellation occurs. The last term of eq. (14) includes the image contribution and describes a dipole source with axis parallel to the surface, Figure 3(b) illustrates in an elementary manner the combination of these various sources.

Our solution to eq. (1) thus reduces to the sum of a volume integral describing longitudinal quadrupoles and a surface integral describing dipoles, i.e.,

$$p(r,t) = \frac{\rho\cos^2\theta}{2\pi rc^2}\frac{\partial^2}{\partial t^2}\iiint_V u_1^2(\eta_i, t-r/c)dV(\eta_i) + \frac{\cos\theta}{2\pi rc}\frac{\partial}{\partial t}\iint_S \tau_0(\eta_i, t-r/c)dS(\eta_i). \quad (15)$$

As pointed out in the INTRODUCTION, we can expect the dipole contribution of eq. (15) to be of the order M^{-2} more efficient than the quadrupole contribution. As a first approximation, we would like to accept this supposition, and examine in detail

$$p(r,t) \simeq \frac{\cos\theta}{2\pi rc}\frac{\partial}{\partial t}\iint_S \tau_0(\eta_i, t-r/c)dS(\eta_i), \quad (16)$$

when $M << 1$.

C. Proposed Model for the Wall Shear Stress Fluctuations

We have developed the solution given by eq. (16) upon the notion that it is the intermittency of the boundary layer within the transition zone that creates noise. Intermittent boundary-layer flow is a situation where we can construct a mathematical model for the fluctuating physical parameters of interest. This model is analogous to that which the

experimentalist uses to distinguish time intervals when his sensor is in irrotational fluid from those when it is in turbulent fluid. Clearly, this is a zero-one function which we shall call the indicator function, $I(x_i,t)$. The use of such a function to describe intermittently turbulent flows is not new, viz., Refs. [16-18], among others. However, as will become apparent below, we will require the space-time correlation functions of $I(x_i,t)$, and these functions have not been so well investigated for boundary-layer transition [19].

Typically, the indicator function at a given point, x_i, in the source volume may be illustrated as in Fig. 4(a). This function is zero when the flow is laminar and is unity when turbulent. Also shown in this illustration is the first time derivative of $I(x_i,t)$ which is a random sequence of alternating Delta functions. Because eq. (16) needs only to be evaluated on the surface, the functional dependence of I on x_2 is not required. It is reasonable to let I be statistically homogeneous in x_3 because of our infinite plane surface assumption; however, I must necessarily be non-homogeneous in x_1.

The non-homogeneity of I in the x_1-direction is due to the fact that the boundary layer ultimately changes from fully laminar to fully turbulent. As x_1 increases beyond x_0 more and more impulse functions fill in the time scale. The time-average value of $I(x_1,t)$ is appropriately called the intermittency factor, i.e.,

$$\gamma(x_1) = \lim_{T\to\infty} \frac{1}{T} \int_0^T I(x_1,t)dt, \tag{17}$$

and represents the fraction of time that the flow is turbulent. This is

a predictable function for boundary-layer transition on flat plates [9] as well as for axisymmetric bodies [20]. Another important mean property of $I(x_1,t)$ is the "burst frequency", $N(x_1)$. This function describes the expected number of bursts that occur at a given point per unit time. It too, may be predicted for most hydrodynamic flows [9, 11, 20]. Figure 5 shows, in principle, how the indicator function varies in time and space; also shown are typical distributions of γ and N.

With these definitions for $I(x_i,t)$, and its mean properties, we propose that

$$\tau_0(x_i,t) = [1-I(x_i,t)]\ \tau_L(x_i) + I(x_i,t)\ \tau_T(x_i) \qquad (18)$$

where i may take on the values 1 and 3. By taking the time derivative of eq. (16) inside the integrals, we find:

$$\frac{\partial \tau_0}{\partial t} = (\tau_T-\tau_L)\ \frac{\partial I}{\partial t} = \sigma(x_i)\ \dot{I}(x_i,t), \qquad (19)$$

where σ was first defined in eq. (6).

At this point it is important to emphasize that eq. (18) implies that the wall shear stress is capable of changing from a laminar value to a turbulent value in an infinitesimally-short period of time ($\dot{I}$'s are Delta functions). Obviously, this would seem physically impossible. However, we do know, from oscillograph traces of the velocity and/or pressure fluctuations that occur in transition flows, that the flow state can change in extremely short periods of time as turbulent bursts are created at or swept by the measuring sensor [10-12]. Equation (18), although idealistic, may be quite adequate for estimating the low-frequency portion of the radiated noise spectrum. The techniques developed by Schottky [21] in his classic analysis of shot noise would seem appropriate here.

At the higher end of the noise spectrum, corresponding to frequencies whose periods are comparable to the actual time required for the wall shear stress to change from a laminar to a turbulent value (or visa versa), we have to take account of the duration and shape of the individual pulses. That is, we must replace the sequence of Delta functions of Fig. 4(a) with some other sequence, $\tilde{\dot{I}}$, as depicted in Fig. 4(b). The time, t_i, represents the short lag time required for the shear stress to change from one regime to another. According to Stratonovich [22], we can solve for the noise spectrum using a random-point process description such as eq. (19) and then modify the result by multiplying by a "frequency-depression factor". This factor is nothing more than the square of the magnitude of the Fourier transform of the individual pulse shape. The details of this procedure will be discussed in Section II.F.

As a final point regarding eq. (18), we note that its time average is simply:

$$\langle \tau_0(x_1,t) \rangle = [1-\gamma(x_1)]\ \tau_L(x_1) + \gamma(x_1)\ \tau_T(x_1) \qquad (20)$$

which is identical to that suggested by Emmons [9] for the transition region. Several experiments have verified this equation, e.g., Dhawan and Narasimha [23].

D. Power Spectral Density of the Radiated Noise

After the substitution of eq. (19) into eq. (16), the radiated acoustic pressure becomes:

$$p(r,t) = \frac{\cos\theta}{2\pi rc} \int_0^{\Delta x} \int_{-\infty}^{\infty} \dot{I}(\eta_1,\eta_3,t-r/c)\ \sigma(x_0+\eta_1)\ d\eta_1 d\eta_3, \qquad (21)$$

where the origin of our coordinate system has been displaced x_0-units downstream in order to simplify the variables in our integrals. The power spectrum can be calculated from the Fourier integral:

$$G(r,\omega) = 4\int_0^\infty \langle p(r,t)\ p(r,t+\tau)\rangle \cos \omega\tau\ d\tau, \tag{22}$$

where $\langle p(r,t)\ p(r,t+\tau)\rangle$ is the autocorrelation function of $p(r,t)$. In general,

$$\langle gg'\rangle \equiv \langle g(t)\ g(t+\tau)\rangle = \lim_{T\to\infty} \frac{1}{T}\int_0^T g(t)\ g(t+\tau)dt. \tag{23}$$

Therefore, for $p(r,t)$:

$$\langle pp'\rangle = \frac{\cos^2\theta}{4\pi^2 r^2 c^2}\iiiint \langle \dot{I}(\eta_1,\eta_3,t-r/c)\ \dot{I}(\phi_1,\phi_3,t-r/c+\tau)\rangle \cdot\sigma(x_0+\eta_1)\ \sigma(x_0+\phi_1)\ d\eta_1 d\eta_3\ d\phi_1 d\phi_3, \tag{24}$$

where for the time being, we will not show the limits of integration. It will prove useful to change the ϕ_i-variables to spatial-separation variables $\xi_i = \phi_i - \eta_i$, such that eq. (24) becomes:

$$\langle pp'\rangle = \frac{\cos^2\theta}{4\pi^2 r^2 c^2}\iiiint \langle \dot{I}(\eta_1,\eta_3,t-r/c)\ \dot{I}(\eta_1+\xi_1,\eta_3+\xi_3,t-r/c+\tau)\rangle \cdot\sigma(x_0+\eta_1)\ \sigma(x_0+\eta_1+\xi_1) d\eta_1 d\eta_3\ d\xi_1 d\xi_3. \tag{25}$$

If we assume $\dot{I}(x_i,t)$ to be stationary in time and homogeneous in x_3, eq. (25) may be written without any loss of generality as:

$$\langle pp'\rangle = \frac{\cos^2\theta}{4\pi^2 r^2 c^2}\iiiint \langle \dot{I}(\eta_1,0,0)\ \dot{I}(\eta_1+\xi_1,\xi_3,\tau)\rangle \cdot\sigma(x_0+\eta_1)\ \sigma(x_0+\eta_1+\xi_1)\ d\eta_1 d\eta_3\ d\xi_1 d\xi_3 \tag{26}$$

The function $\langle \dot{I}\dot{I}' \rangle$ in this equation is the space-time correlation function for the first time derivative of our indicator function. Unfortunately, this function has not been investigated in enough detail for us to set down an explicit expression for it.

In order to continue the analysis, however, we will assume (as Corcos [24] did for fully-developed turbulent flow) that $\langle \dot{I}\dot{I}' \rangle$ can be separated. The separation technique we will use, although somewhat heuristic, is based on our physical notions of the transition process. Let us write:

$$\langle \dot{I}\dot{I}' \rangle = R_3(\xi_3)\, \tilde{R}_1(\eta_1)\, \tilde{R}(\tau - \xi_1/u_c), \tag{27}$$

where $R_3(\xi_3)$ represents the spanwise correlation function for the bursts. It would seem reasonable that R_3 is also a function of η_1. We develop this dependence by writing the integral of eq. (26) which is over ξ_3; namely,

$$\int_{-\infty}^{\infty} R_3 d\xi_3 = \int_{-L_3}^{L_3} d\xi_3 = 2L_3(\eta_1), \tag{28}$$

where L_3 is the transition-width integral scale. Chen and Thyson [20] discuss a spanwise length scale in the region of transition where the bursts begin to overlap; that is, where $\eta_1 \to \Delta x$. They write this scale in the form

$$\Lambda \simeq 1.5\, \Delta x \tan \alpha. \tag{29}$$

Let us set $L_3(\Delta x) = \Lambda$ and $L_3(0) = 0$. It would then seem that

$$L_3(\eta_1) \simeq 1.5 \eta_1 \tan \alpha \tag{30a}$$

$$\simeq \eta_1/4 \quad \text{for} \quad \alpha = 9.6°. \tag{30b}$$

The second two factors of eq. (27) represent the time autocorrelation function of $\dot{I}(\eta_1,t)$ at a fixed point in the transition zone, η_1. In particular,

$$\tilde{R}_1(\eta_1)\tilde{R}(\Delta) = \langle \dot{I}(\eta_1,t)\ \dot{I}(\eta_1,t+\Delta)\rangle, \tag{31}$$

where $\Delta = \tau - \xi_1/u_c$ accounts for the added time delay due to the convection of a turbulent burst over the distance $(\eta_1+\xi_1) - \eta_1$. It is noted that this covariance is written in a form suggesting that $\tilde{R}_1$ is the standard deviation of $\dot{I}(t)$ at η_1 and that $\tilde{R}$ is the normalized autocorrelation function of $\dot{I}$ at the same point. These particular moments of $\dot{I}$ can be estimated if we assume a given probability density function for the temporal process. Before doing this, however, let us make use of the fact that

$$\langle \ddot{I}I' \rangle = -\frac{\partial^2}{\partial\Delta^2}\langle II' \rangle \tag{32}$$

such that (Stratonovich, ibid., p. 170) the power spectrum for a point process composed of Delta functions is equivalent to ω^2 times the power spectrum of the same process composed of unit impulse functions. Consequently, eq. (22), after using eq.'s (28) and (30b), can be written as:

$$G(r,\omega) = \frac{\omega^2\cos^2\theta}{2\pi^2 r^2 c^2}\int_0^\infty \cos\omega\tau \iiint \eta_1\sigma(x_0+\eta_1)\ \sigma(x_0+\eta_1+\xi_1)$$

$$\cdot\ R_1(\eta_1)\ R(\tau-\xi_1/u_c)\ d\eta_1 d\eta_3\ d\xi_1 d\tau, \tag{33}$$

where now

$$R_1(\eta_1)\ R(\Delta) = \langle I(\eta_1,t)\ I(\eta_1,t+\Delta)\rangle. \tag{34}$$

The standard deviation for our indicator function, $I(\eta_1,t)$ is the intermittency factor, $\gamma(\eta_1)$, since by eq. (17)

$$\gamma(\eta_1) = \lim_{T\to\infty} \frac{1}{T} \int_0^T I(\eta_1,t)dt = \lim_{T\to\infty} \frac{1}{T} \int_0^T I^2(\eta_1,t)dt.$$

Thus, we let

$$R_1(\eta_1) = \gamma(\eta_1). \tag{35}$$

In regards to $R(\Delta)$, we let the random sequence of impulse functions that make up our indicator function be Poisson distributed. We select this distribution because it is a discrete distribution (which it necessarily must be) for a number of events (turbulent bursts) that all happen at random times with an average of N events per unit time (our burst frequency). Indeed, the experimental investigation of turbulence bursts by DeMetz, et.al. [25] does suggest a Poisson process. Under this assumption, the classical correlation function for a random telegraph signal may be used (see Rice [26]) for $R(\Delta)$, i.e.,

$$R(\Delta) = e^{-2N(\eta_1)|\Delta|}. \tag{36}$$

Differentation of eq. (33) with respect to x_3 gives the power spectrum of the acoustic pressure radiated per unit spanwise width of transition. We find:

$$\frac{\partial G(\omega,\mathbf{r})}{\partial x_3} = \frac{\omega^2\cos^2\theta}{2\pi^2 r^2 c^2} \int_0^{\Delta x} \eta_1\gamma(\eta_1)\ \sigma(x_0+\eta_1) \int_{-\eta_1}^{\Delta x-\eta_1} \sigma(x_0+\eta_1+\xi_1)$$

$$\cdot \left\{ \int_0^\infty \exp[-2N(\tau-\xi_1/u_c)]\ \cos\omega\tau d\tau \right\} d\xi_1 d\eta_1, \tag{37}$$

where the integral in braces is immediately recognized as the Laplace transform of $\cos\omega\tau$. Because

$$\mathcal{L}[\cos\omega\tau] = \frac{s}{s^2+\omega^2} \quad ,$$

with $s = 2N(\eta_1)$, eq. (37) reduces to:

$$\frac{\partial G(r,\omega)}{\partial x_3} = \frac{\omega^2 \cos^2\theta}{\pi^2 r^2 c^2} \int_0^{\Delta x} \eta_1 \sigma(x_0+\eta_1)\gamma(\eta_1) \int_{-\eta_1}^{\Delta x-\eta_1} \frac{N(\eta_1)\sigma(x_0+\eta_1+\xi_1)\exp(2N\xi_1/u_c)}{[4N^2(\eta_1) + \omega^2]}\, d\xi_1 d\eta_1. \quad (3$$

We would like to simplify this double-integral solution another step farther by assuming that $\sigma(=\tau_T-\tau_L)$ is only weakly dependent on its argument. In particular, through a Taylor series expansion of eq.'s (4) and (5), it can be shown that

$$\sigma(x_0+\varepsilon) \simeq Ax_0^{-1/5}\left(1 - \frac{\varepsilon}{5x_0}\right) - Bx_0^{-1/2}\left(1- \frac{\varepsilon}{2x_0}\right), \qquad (39)$$

where

$$A = 0.0288\rho u_0^2 Re_u^{-1/5},$$

$$B = 0.332\rho\nu u_0 Re_u^{1/2},$$

with

$Re_u = u_0/\nu$, which is the unit Reynolds number.

The maximum value which ε assumes is Δx, the streamwise extent of the transition zone. For incompressible boundary-layer transition, Δx can be estimated from the following emperical relationship [20,23] between the Reynolds number based on the transition point, x_0 and that based on Δx:

$$Re_{\Delta x} = 60 Re_t^{2/3}. \qquad (40)$$

This relation can be rewritten in the form

$$\frac{\Delta x}{x_0} = \frac{\varepsilon_{max}}{x_0} = 60 Re_t^{-1/3}.$$

In connection with the discussion following eq. (6), we would expect the first term (the turbulent wall shear stress) of eq. (39) to dominate, so that

$$\sigma(x_0 + \varepsilon_{max}) \simeq Ax_0^{-1/5}(1 - 12Re_t^{-1/3})$$

$$\simeq \sigma(x_0). \tag{41}$$

This approximation implies that if the boundary layer were completely laminar or completely turbulent over the distance Δx, then the mean value of the wall shear stress changes insignificantly over this streamwise distance. It is analogous to the parallel-flow assumption commonly used in analyses related to fully-developed turbulent boundary-layer flow.

Integration of eq. (38) over ξ_1 can now be performed; we find:

$$\frac{\partial G(r,\omega)}{\partial x_3} = \frac{\omega^2 \cos^2\theta\, \sigma^2(x_0) u_c}{2\pi^2 r^2 c^2} \int_0^{\Delta x} \frac{\eta_1 \gamma(\eta_1)}{(4N^2+\omega^2)} \{\exp[2N(\Delta x - \eta_1)/u_c]$$

$$- \exp[-2N\eta_1/u_c]\} d\eta_1. \tag{42}$$

E. Intermittency and Burst Frequency Distributions

In order to perform the final integration of eq. (42), we need the intermittency and burst frequency distributions for transition on a flat plate. Emmons [9] first discussed these distributions and developed a probabilistic model to predict them. He assumed the existence of a source-rate density function, $g(x_0, z_0, t)$, which specifies the rate of production of turbulent point-source bursts per unit area on the surface at position $x_1 = x_0$, $x_3 = z_0$, and time t_0. In his example, Emmons assumed $g(x_0, z_0, t_0)$ to be constant; however, a later investigation by Narasimha [27] which made use of the data of Ref. [10], showed that

$g(x_0,z_0,t_0)$ is more accurately described by a Delta function. In particular, $g(x_1) = n\delta(x_1-x_0)$, where n is defined as the number of sources per unit length per unit time along the line $x_1 = x_0$.

Farabee, et. al. [11] showed that for this assumed form of g:

$$\gamma(\eta_1) = 1-\exp(-\sigma^* n\eta_1^2/u_0), \tag{43}$$

and

$$N(\eta_1) = n\tan(\alpha)\eta_1\exp(-\sigma^* n\eta_1^2/u_0), \tag{44}$$

where

$$\sigma^* = (u_\ell-u_t)u_0\tan\alpha/(u_c u_t). \tag{45}$$

These equations depend upon the characteristic leading and trailing edge velocities of a turbulent burst (Fig. 2), and upon n. The investigators of Ref. [11] performed detailed measurements of the intermittent boundary layer on a flat flat and fit eqs. (43) and (44) to their data. The resulting expressions are as follows:

$$\gamma(\bar{x}_1) = 1-\exp[-4.185\bar{x}_1^2], \tag{46}$$

and

$$N(\bar{x}_1) = 1.272\,\frac{u_0}{\Delta x}\,\bar{x}_1\exp[-4.185\bar{x}_1^2], \tag{47}$$

where

$$\bar{x}_1 = (x_1-x_0)/\Delta x = \eta_1/\Delta x. \tag{48}$$

Figure 6 show these distributions.

We non-dimensionalize the variable of integration in eq. (42) according to eq. (48), and then use eqs. (46) and (47) for $\gamma(\bar{x}_1)$ and $N(\bar{x}_1)$ to obtain:

$$\frac{\partial G(r,\kappa)}{\partial x_3} = \frac{(\kappa\Delta x)^2\cos^2\theta\sigma^2(x_0)u_c(\Delta x)^2}{2\pi^2 r^2 c^2}\,F(\kappa,u_0/u_c), \tag{49}$$

where $\kappa = \omega/u_0$, which is the free-stream convection wavenumber. The frequency function, F, is given by:

$$F(\kappa,\frac{u_0}{u_c}) = \int_0^1 \frac{\{\bar{x}_1-\bar{x}_1\exp(-a\bar{x}_1^2)\}\{\exp[b(\frac{u_0}{u_c})(\bar{x}_1-\bar{x}_1^2)\exp(-a\bar{x}_1^2)]-\exp[-b(\frac{u_0}{u_c})\bar{x}_1^2\exp(-a\bar{x}_1^2)]\}}{b^2\bar{x}_1^2\exp(-2a\bar{x}_1^2) + (\kappa\Delta x)^2}\,d\bar{x}_1, \tag{50}$$

where a = 4.185 and b = 2.544. We have been unable to integrate eq. (50) to closed-form; however, this integral depends only upon the reduced frequency, $\kappa\Delta x$, and the ratio of the free-stream velocity to the convection velocity of turbulent bursts, u_0/u_c. Assuming u_c/u_0 is independent of frequency, this ratio is known [10,11] to fall within the range $0.6 \leq u_c/u_0 \leq 0.8$. Thus, eq. (50) can be numerically-integrated for a few discrete value of u_c/u_0 and a range of $\kappa\Delta x$. We have performed this numerical integration by Simpson's rule. The product $(\kappa\Delta x)^2 F(\kappa, u_0/u_c)$ is presented graphically in Fig. 7 for three typical values of u_c/u_0. This function is seen to be weakly dependent on the convection velocity ratio, rises at 12 dB/octave at low frequencies, and asymptotically approaches a constant for reduced frequencies greater than the characteristic frequency of turbulent bursts. When multiplied by the numerical factor given in eq. (49), Fig. 7 represents the low-frequency radiated noise spectrum for boundary-layer transition of unit spanwise width.

Because $\dot{\sigma}(x_0)$ is proportional to ρu_0^2, and u_c is proportional to u_0, we see that the spectral level is proportional to u_0^5 for constant Δx. However, eq. (40) suggests that Δx is inversely proportional to u_0, so eq. (49) predicts a u_0^3 velocity dependence even though the source of noise is dipole. The reason for this unexpected behavior is that the solution is derived in terms of the detailed hydrodynamics. These details result in a source area that changes with velocity. Thus, to be consistent with less-rigorous, flow noise order of magnitude estimates, the radiation-field pressure should be normalized by the area of the source region, which is proportional to Δx. The mean-square value

of the sound pressure radiated per unit area would then be given by the integration of eq. (49) over frequency divided by $(\Delta x)^2$. A 5th power velocity dependence would thus be retained.

F. Frequency-Depression Factor

As discussed briefly in Section II.C, the power spectral density given by eq. (49) is most valid at frequencies lower than or comparable to the burst frequency associated with turbulent spot formation. At higher frequencies, we must take account of the actual shape and duration of the individual pulses. We do this, by assuming a new indicator function, $\tilde{\tilde{I}}$, as shown in Fig. 4(b). This function depends upon a lag time, t_i, which represents the time it takes for the wall shear stress to change from a laminar value to a turbulent value. We will assume that the time required for the turbulent wall shear stress to return to a laminar value is also given by t_i. Thus, we assume a symmetrical pulse shape. With reference to Stratonovich [22], we simply need to multiply eq. (49) by a frequency-depression factor, given in general by:

$$|J(i\omega)|^2 = \left|\int_{-\infty}^{\infty} \tilde{\tilde{I}} e^{-i\omega t} dt\right|^2 . \tag{51}$$

Letting $\tilde{\tilde{I}} \sim V_0 e^{-t/t_i}$, where $V_0 \sim t_i^{-1}$, e.g. Skudrzyk [28], it is easy to show that

$$|J(i\omega)|^2 = [1+(\omega t_i)^2]^{-1} . \tag{52}$$

It is apparent that when eq. (49) is multiplied by eq. (52), the spectrum will roll of at 12 dB/octave above those frequencies inversely proportional to t_i. The spectral shape of the radiated noise is therefore

analogous to the one we obtain by passing white noise through a realizable bandbass filter. The low-frequency cutoff is predicted by the present theory, but the high-frequency cutoff can only be estimated since there is very little information regarding the magnitude of t_i. We expect though, that t_i would be on the order of fractions of a millisecond, and it probably depends on the Reynolds number, the flow velocity, and perhaps even on the kinematic viscosity.

III. EXAMPLES

We now consider application of the present analysis to two independent experimental situations where boundary-layer flow noise was measured; namely, those of Refs. [2] and [3]. Both of these experimental investigations were performed in water at Mach numbers less than 0.02, which is of the proper order of magnitude for our noise model. They used axisymmetric bodies and concentrated on measuring the radiating component of flow noise through the utilization of relatively large flush-mounted hydrophones and distant receivers. The data of Ref. [2] were collected in a large lake with a buoyantly-propelled vehicle equipped with a hemispherically-shaped nose. The investigation performed by the author [3] used a blunt, flat-faced nose body designed to operate in a large water tunnel. Calculations performed for both headforms indicate that laminar separation is likely to occur at the test velocities used. From hot-film anemometry studies, the transition from laminar-to-turbulent flow was found to occur at the predicted point of separation on the water tunnel body. Downstream of that point, oscilloscope traces of the hot film signals indicated that turbulent bursts did appear, but Δx was very short, and essentially constant ($\Delta x \simeq 0.1D$, where D = body diameter) over the range of velocities considered.

We assume, since measurements were not reported, that the transition zone for the hemispherical nose of Haddle and Skudrzyk's buoyant body [2] would exhibit similar behavior, i.e., $\Delta x \simeq 0.1D$.

Let us first apply eq. (49) to typical flow noise spectra reported in Ref. [3]. We choose a hydrophone location that is away from both the transition and fully-developed turbulent regions of the body. We further restrict this location to be in a region where noise eminating from the transition zone is minimally affected by diffraction due to the nose curvature. Hydrophone location 6 [Lauchle, ibid., Fig. 10(a)] best meets these criteria; it is 7.62 cm. forward of the transition point within the laminar boundary layer. We thus set $r=7.62$ cm., $\theta=0°$, and the spanwise width of the transition zone equal to the body circumference.

The rise time, t_i, can only be estimated. We have examined under a microscope the oscilloscope traces of the signals from very small pinhole microphones placed in the intermittent boundary-layer flow of a flat plate [25]. Microphone data were selected over hot wire or film data because of the higher frequency response. From this examination, we crudely selected 0.25 msec. as the time required for the signal characteristics to change as a turbulent burst swept by the sensor.

With $\Delta x=3.42$ cm., $u_c/u_0=0.7$ and r, θ, and t_i set at the above noted values, the spectra predicted by eq. (49) (together with the frequency-depression factor) for $u_0=7.62$ and 10.67 m./sec. are compared with those determined experimentally in Fig. 8. The correlation below about 10 kHz appears to be good. The high-frequency portions of the measured spectra may include contributions from additional noise sources, such as the fully-

developed turbulent flow over the body, or the unsteady secondary flows that occur at the body mounting strut junctures.

Vecchio and Wiley [29] developed a theory for the noise radiated by a fully-developed turbulent boundary layer. They compared their prediction with the radiated noise spectrum of Haddle and Skudrzyk's [ibid., Fig. 19] wooden buoyant body. This experimental spectrum was measured about 30 m. away from the buoyant unit rising at 15.44 m./sec. Their prediction underestimates the radiated sound for frequencies less than about 2 kHz, but agrees quite well with the experimental levels at higher frequencies.

As our second example, we apply the present theory for transition zone radiated noise to this experimental situation. We let r be the radius of a sphere whose surface area is the same as the surface area of the body [2,29], and as in the first example, we let $\Delta x = 0.1D$, where D is 48.26 cm. for this particular buoyant body. With t_i=0.25 msec., our prediction is shown in Fig. 9 along with that prediction for the noise generated by the fully-developed turbulent boundary that occurs on the body [Vecchio and Wiley, ibid., Fig. 1]. It appears that the levels predicted for transition fill in that portion of the spectrum where the theory for fully-developed turbulent flow underpredicts. Indeed, if we assume the two noise sources are uncorrelated, we can add the energies and obtain a composite spectrum as shown in Fig. 9. This composite agrees very well with the measured spectrum.

IV. SUMMARY AND RECOMMENDATIONS

We have presented an analysis of the radiated sound due to boundary-

layer transition. Our principle assumptions were that the surface is infinite in extent, planar, and rigid, that the transition process includes a finite region intermittent flow where the boundary layer fluctuates randomly between laminar and turbulent, and that it is this intermittent flow that generates the noise. Through use of Lighthill's analogy, we showed that the fluctuations between laminar and turbulent boundary-layer flow give rise to dipole, quadrupole, and octupole noise sources. On the basis of a very low Mach number assumption, we treated only the dipole contribution in detail. We assumed that the flow is statistically homogeneous in the spanwise directions, non-homogeneous in the streamwise direction, and stationary, but Poisson distributed in time. The power spectral density for the acoustic pressure radiated per unit spanwise width was derived. The level of the mean-square radiated pressure was found to depend upon the square of the difference between the turbulent wall shear stress and the laminar wall shear stress that would occur at the beginning of transition, upon the square of the streamwise distance over which turbulent bursts occur, and upon the velocity at which turbulent bursts are convected along the surface. The spectral shape corresponds to that obtained by passing white noise through a realizable bandpass filter with low and high frequency cutoffs dependent upon the characteristic frequency of turbulent spot formation and the time required for the wall shear stress to change from a locally laminar (or turbulent) to a locally turbulent (or laminar) value, respectively.

We compared predictions using this theory with available experimental data and observed rather good agreement. As expected, we observed better

agreement if the acoustic energy generated by the fully developed turbulent motion over the given experimental vehicle was added to the acoustic energy generated by transition. This agreement suggests that the present analysis is applicable to axisymmetric bodies providing that the sound wavelength is large and that the source region is small relative to the body radii of curvature.

The analysis presented here represents a rigorous effort to include the detailed hydrodynamics into an estimate for the sound generated by boundary-layer transition. The resulting expression for this sound defines two hydrodynamic parameters that critically control the level and spectrum of the sound generated; namely, Δx and t_i. As Δx becomes smaller, we find that less noise is generated at the same value of free-stream velocity. It is recommended that experimental investigation of this dependence be considered, i.e., previous efforts have not included Δx as a test variable. If Δx is verified to be a controlling parameter of the radiated noise, then various schemes of boundary-layer control to minimize Δx, while at the same time being inherently quiet themselves, might be proposed.

There have been no known analytical or experimental studies specifically directed toward the determination of the time it takes for the wall shear stress to change state. This time, t_i, plays an important role in the high-frequency part of the noise spectrum. The larger t_i is, the lower the frequency at which the noise spectrum begins to roll off. We might expect that t_i scales with the turbulent velocities very near and normal to the surface; these velocities scale with the friction velocity, u_*. The viscous sub-layer thickness, Θ, identifies that region where $\partial u_1/\partial x_1$ is essentially constant. Therefore, t_i may be proportional to Θ/u_*. As discussed by

Tennekes and Lumley [30], the Reynolds number, $Re_\Theta = \Theta u_*/\nu$, is small, falling in the range 10-100. With $u_* \sim u_0/30$, we find:

$$t_i \sim 900\ Re_\Theta\ \nu/u_0^2 \quad . \tag{53}$$

For $Re_\Theta = 30$, and water flow at 10 m./sec., t_i is calculated to be of the order 0.2 msec. which compares very well with our crude estimate based on oscillograph observations. From this dimensional reasoning, it appears that t_i depends upon ν and u_0. We need to establish, however, a more precise value for Re_Θ during the initial stages of turbulent boundary-layer flow. Carefully designed experiments in both air and water, which utilize high-frequency response sensors (pressures sensors may be best suited for this) may provide a data base for t_i. Equation (53) could serve as a data scaling relation from which Re_Θ may be deduced.

REFERENCES

[1] Ffowcs Williams, J.E., "Flow Noise," in: Underwater Acoustics (V.M. Albers, ed.) Vol. 2, Plenum Press, New York, 1967, p. 89.

[2] Haddle, G.P. and Skudrzyk, E.J., "The Physics of Flow Noise," J. Acoust. Soc. Am., Vol. 46, pp. 130-157, 1969.

[3] Lauchle, G.C., "Noise Generated by Axisymmetric Turbulent Boundary-Layer Flow," J. Acoust. Soc. Am.,Vol. 61, pp. 694-703, 1977.

[4] Dolgova, I.I., "Sound Field Radiated by a Tollmien - Schlichting Wave," Sov. Phys. Acoust., Vol. 23, pp. 259-260, 1977.

[5] Brooke Benjamin, T., "The Development of Three-Dimensional Disturbances in an Unstable Film of Liquid Flowing Down an Inclined Plane," J. Fluid. Mech., Vol. 10, pp. 401-419, 1961.

[6] Lighthill, M.J., "On Sound Generated Aerodynamically, II: Turbulence as a Source of Sound," Proc. Roy. Soc. Lond. A222, pp. 1-32, 1954.

[7] Landahl, M.T., "Wave Mechanics of Boundary Layer Turbulence and Noise," J. Acoust. Soc. Am., Vol. 57, pp. 824-831, 1975.

[8] Ross, D., Mechanics of Underwater Noise, Pergamon Press, New York, 1976, p. 51.

[9] Emmons, H.W., "The Laminar-Turbulent Transition in a Boundary Layer - Part I," J. Aero. Sci., Vol. 18, No. 7, pp. 490-498, 1951.

[10] Schubauer, G.B. and Klebanoff, P.S., "Contributions on the Mechanics of Boundary Layer Transition," NACA Rept. 1289, 1956.

[11] Farabee, T.M., Casarella, M.J. and DeMetz, F.C., "Source Distribution of Turbulent Bursts During Natural Transition," David W. Taylor Naval Ship Research and Development Center Report SAD-89E-1942, August 1974.

[12] Schlichting, H., Boundary-Layer Theory, 6th Ed., McGraw-Hill Book Co., New York, 1968, pp. 598, 128.

[13] Lu, S. S., and Willmarth, W. W., "Measurements of the Structure of the Reynolds Stress in a Turbulent Boundary Layer," J. Fluid Mech., Vol. 60, pp. 481-511, 1973.

[14] Curle, N., "The Influence of Solid Boundaries Upon Aerodynamic Sound," Proc. Roy. Soc. Lond. A231, pp. 505-514, 1955.

[15] Powell, A., "Aerodynamic Noise and the Plane Boundary," J. Acoust. Soc. Am., Vol. 32, pp. 982-990, 1960.

[16] Kovasznay, L.S.G., Kibens, V. and Blackwelder, R.F., "Large-scale Motion in the Intermittent Region of a Turbulent Boundary Layer," J. Fluid Mech., Vol. 41, pp. 283-325, 1970.

[17] Libby, P.A., "On the Prediction of Intermittent Turbulent Flows," J. Fluid Mech., Vol. 68, pp. 273-295, 1975.

[18] Lessmann, R.C., "Intermittent Transition Flow in a Boundary Layer," AIAA J., Vol. 15, pp. 1656-1658, 1977.

[19] Kovasznay, et. al., ibid., p. 308, investigated the space-time correlation functions for $I(x_2,t)$ that occurs through the outer shear flow area of fully-developed turbulent flow. These results are not directly applicable to the present analysis.

[20] Chen, K.K. and Thyson, N.A., "Extension of Emmons' Spot Theory to Flows on Blunt Bodies," AIAA J., Vol. 9, pp. 821-825, 1971.

[21] Schottky, W., "Theory of Shot Effect," Ann. Phys., Vol. 57, pp. 541-568, 1918.

[22] Stratonovich, R.L., Topics in the Theory of Random Noise, Volume I, Gordon and Breach Science Publ., New York, 1963, p. 157.

[23] Dhawan, S. and Narasimha, R., "Some Properties of Boundary Layer Flow During the Transition From Laminar to Turbulent Motion," J. Fluid Mech., Vol. 3, pp. 418-436, 1958.

[24] Corcos, G.M., "Resolution of Pressure in Turbulence," J. Acoust. Soc. Am., Vol. 35, pp. 192-199, 1963.

[25] DeMetz, F.C. and Casarella, M.J., "An Experimental Study of the Intermittent Properties of the Boundary Layer Pressure Field During Transition on a Flat Plate," David W. Taylor Naval Ship Research and Development Center Report 4140, AD-775-299, Nov. 1973.

[26] Rice, S.O., "Mathematical Analysis of Random Noise," Bell Sys. Tech. J., Vol. 23, pp. 282-332, 1944.

[27] Narasimha, R., "On the Distribution of Intermittency in the Transition Region of a Boundary Layer," J. Aero. Sci., Vol. 24, pp. 711-712, 1957.

[28] Skudrzyk, E., The Foundations of Acoustics: Basic Mathematics and Basic Acoustics, Springer-Verlag, New York, 1971, p. 90.

[29] Vecchio, E.A. and Wiley, C.A., "Noise Radiated from a Turbulent Boundary Layer," J. Acoust. Soc. Am., Vol. 53, pp. 596-601, 1973.

[30] Tennekes, H. and Lumley, J. L., A First Course in Turbulence, The MIT Press, Cambridge, 1972, Chapter 5.

July 28, 1978
GCL:jrp

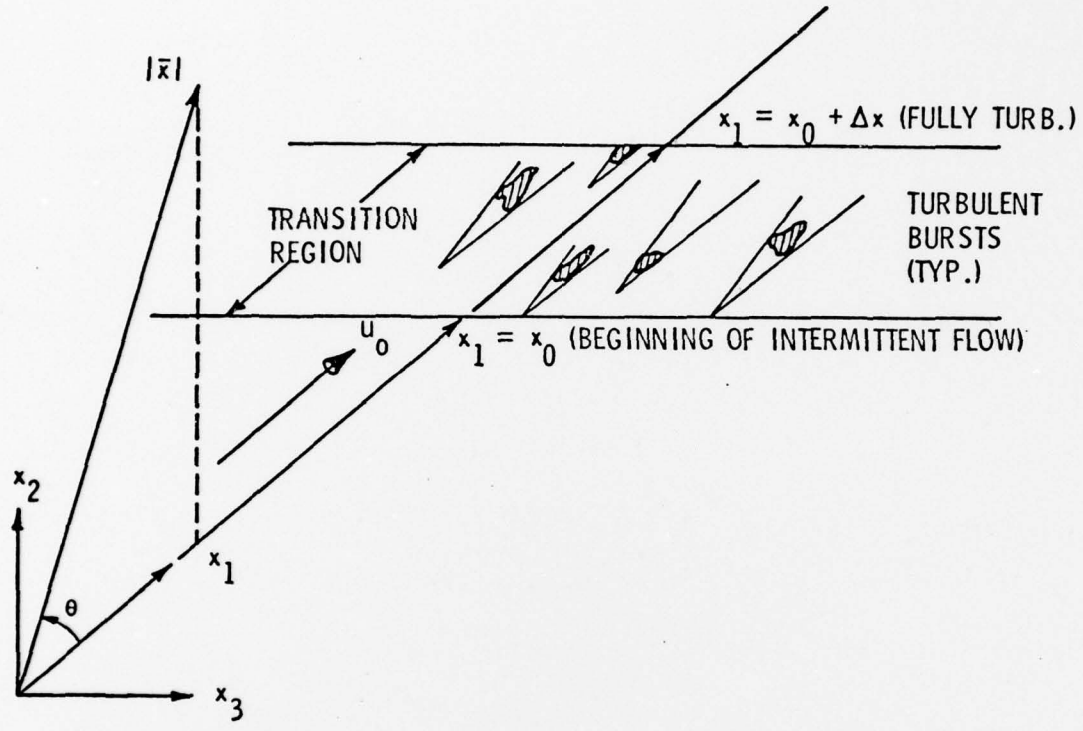

Figure 1. Definition of the coordinates used and a schematic representation of the transition process.

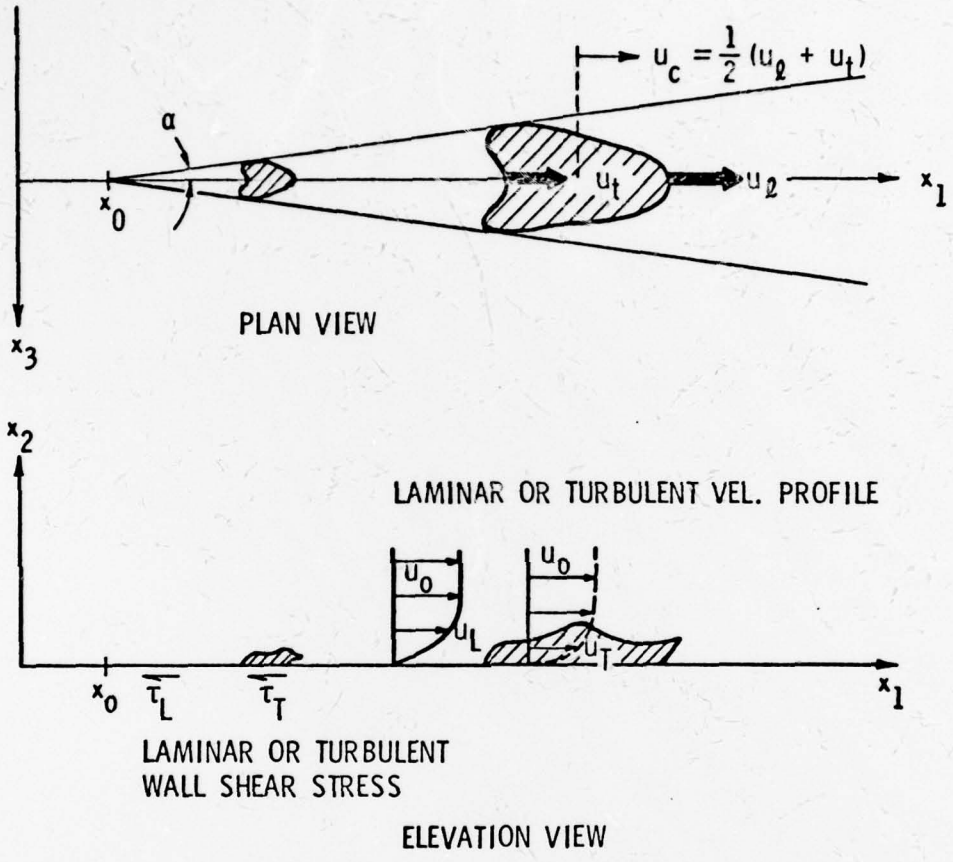

Figure 2. Schematic description of turbulent bursts and the boundary layer development.

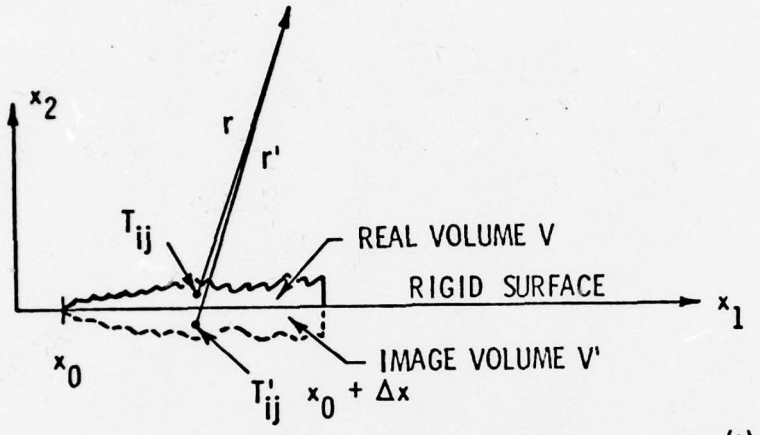

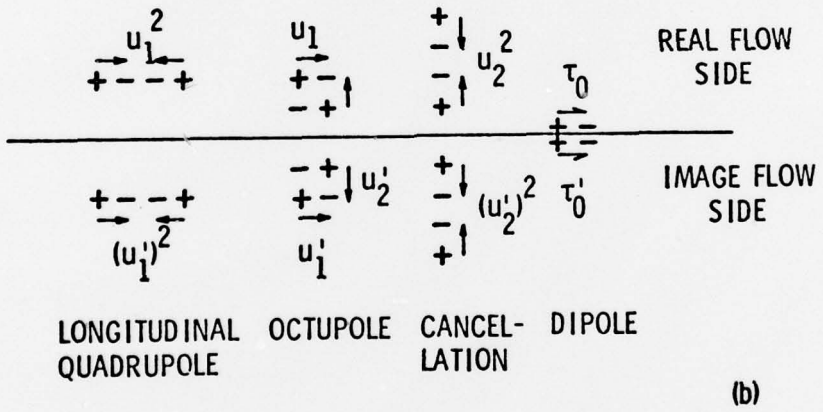

Figure 3. (a) A schematic representation of the image flow concept; and (b) the way in which multipole sources in the real flow combine with equivalent sources in the image flow.

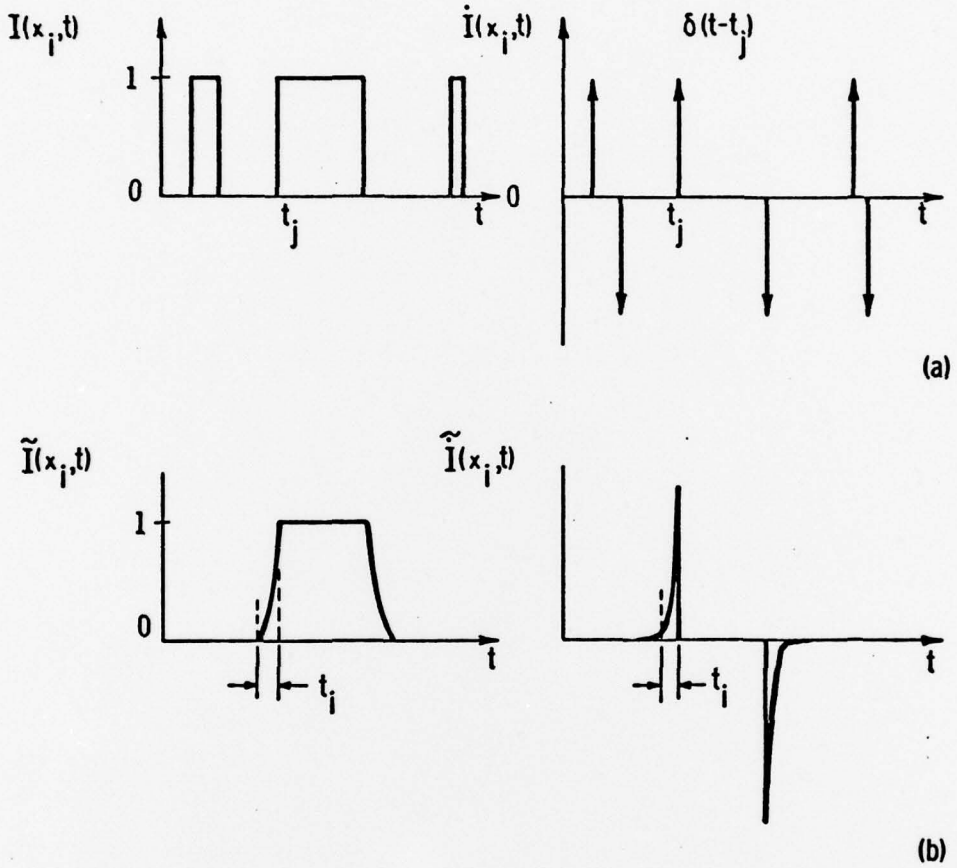

Figure 4. (a) An idealistic indicator function composed of unit impulse functions and its first time derivative; and, (b) a more realistic form of the indicator function and its derivative

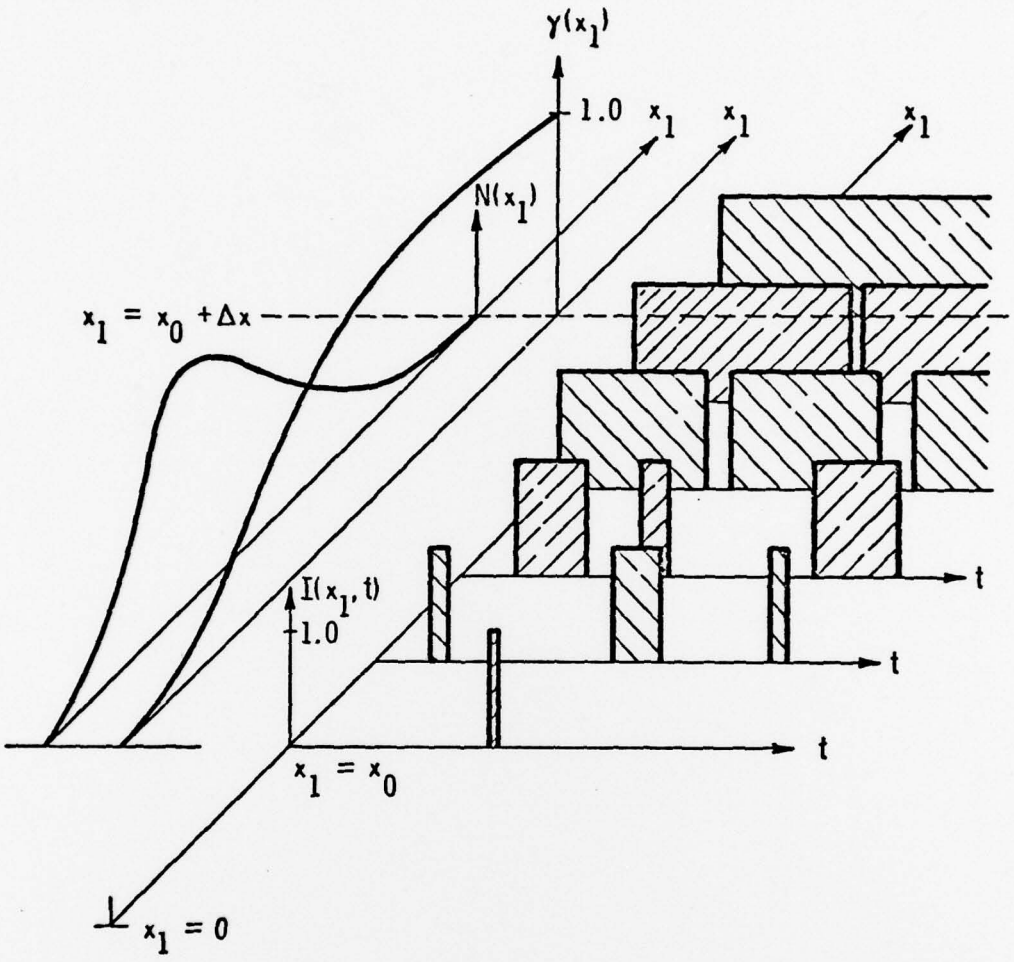

Figure 5. A schematic representation of $I(x_1,t)$ in space and time, where γ is its time average value and N is the expected number of bursts per unit time.

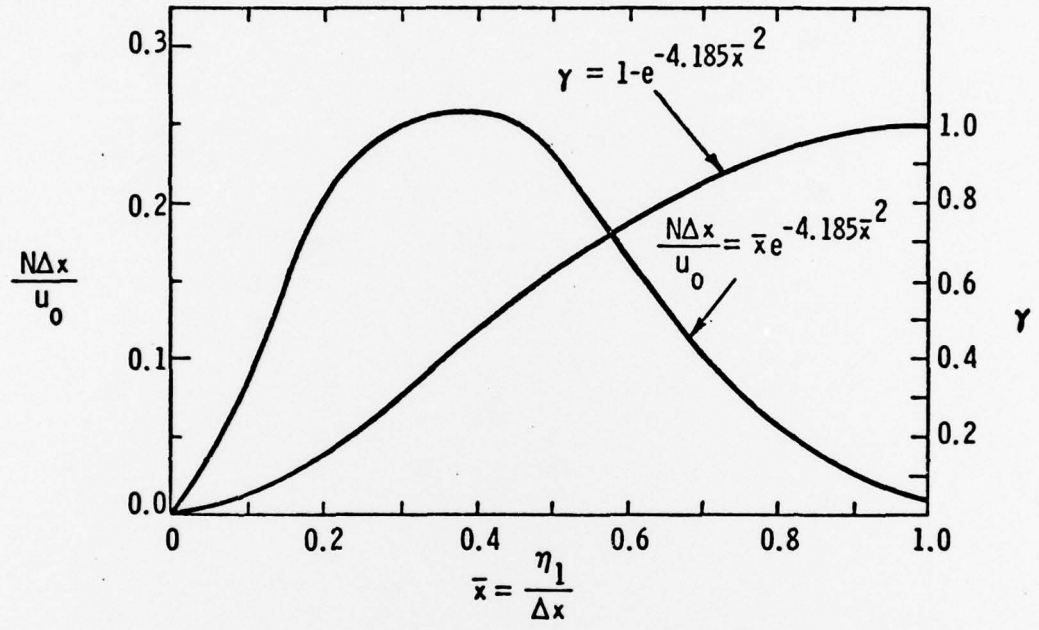

Figure 6. The intermittency and burst frequency distributions from Farabee, et al. [11]

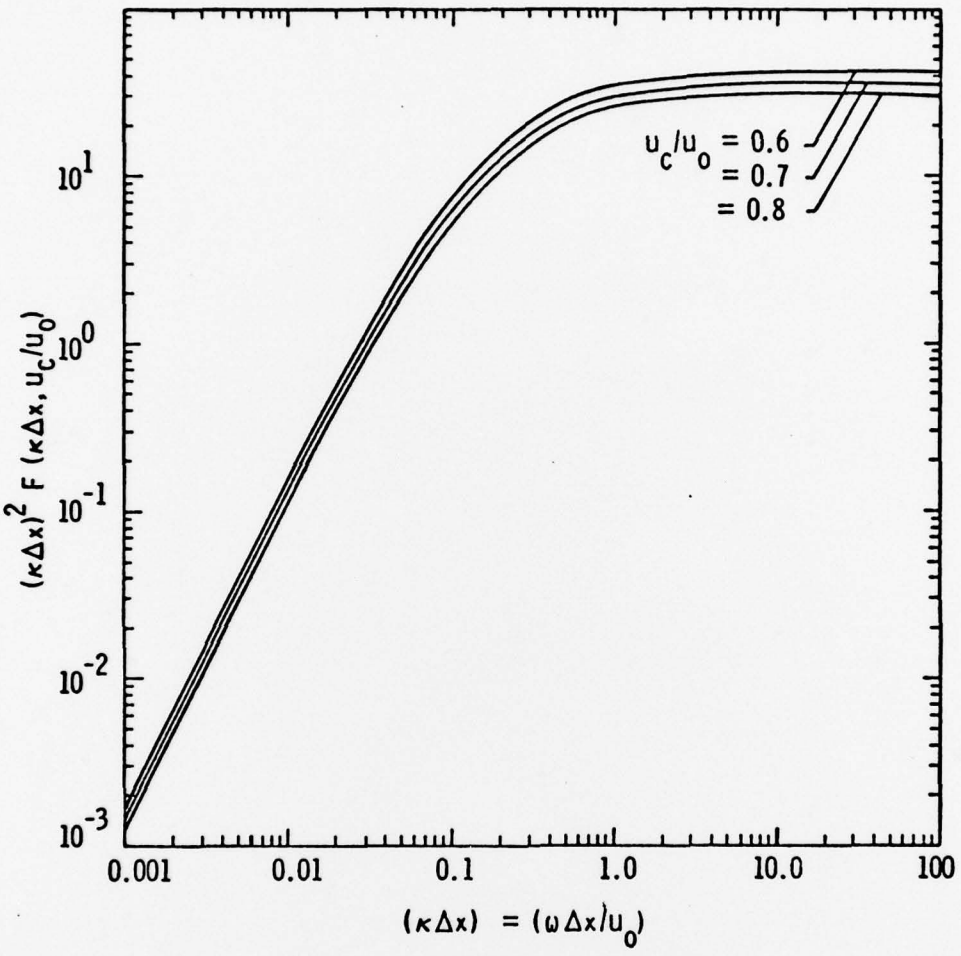

Figure 7. Graphical presentation of the frequency integral given by eq. (50).

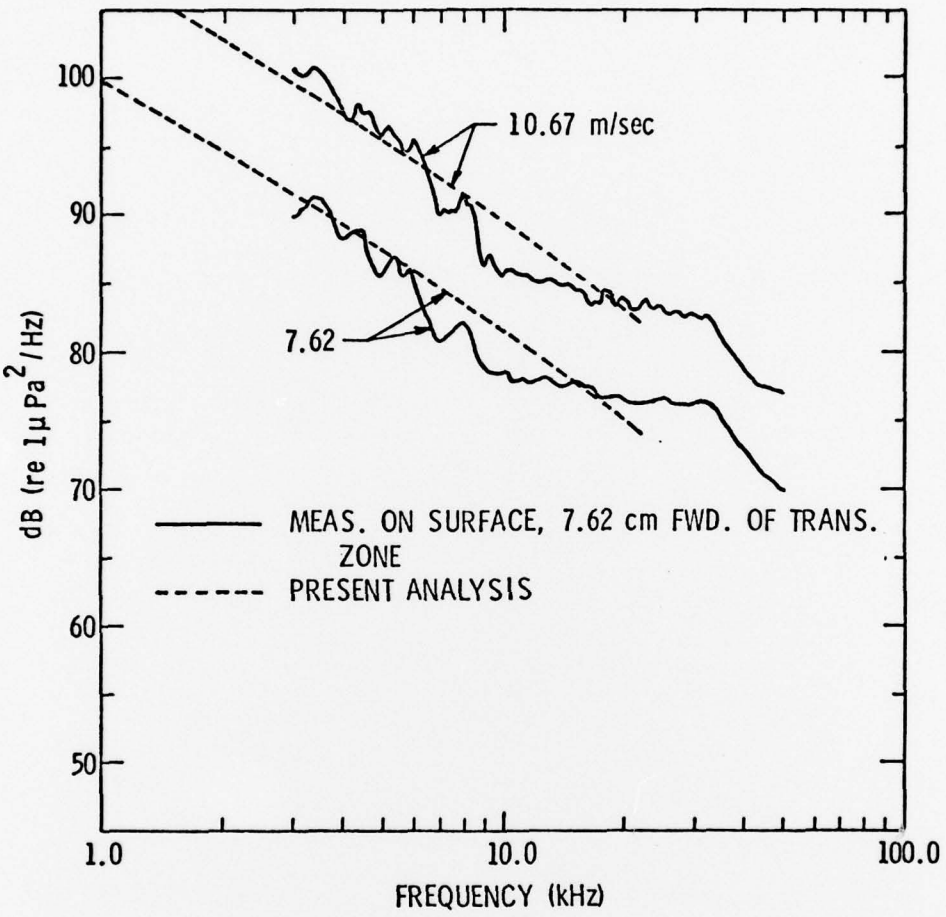

Figure 8. Comparison of the theory with experimental spectra measured on the surface of a water tunnel flow noise research vehicle [3].

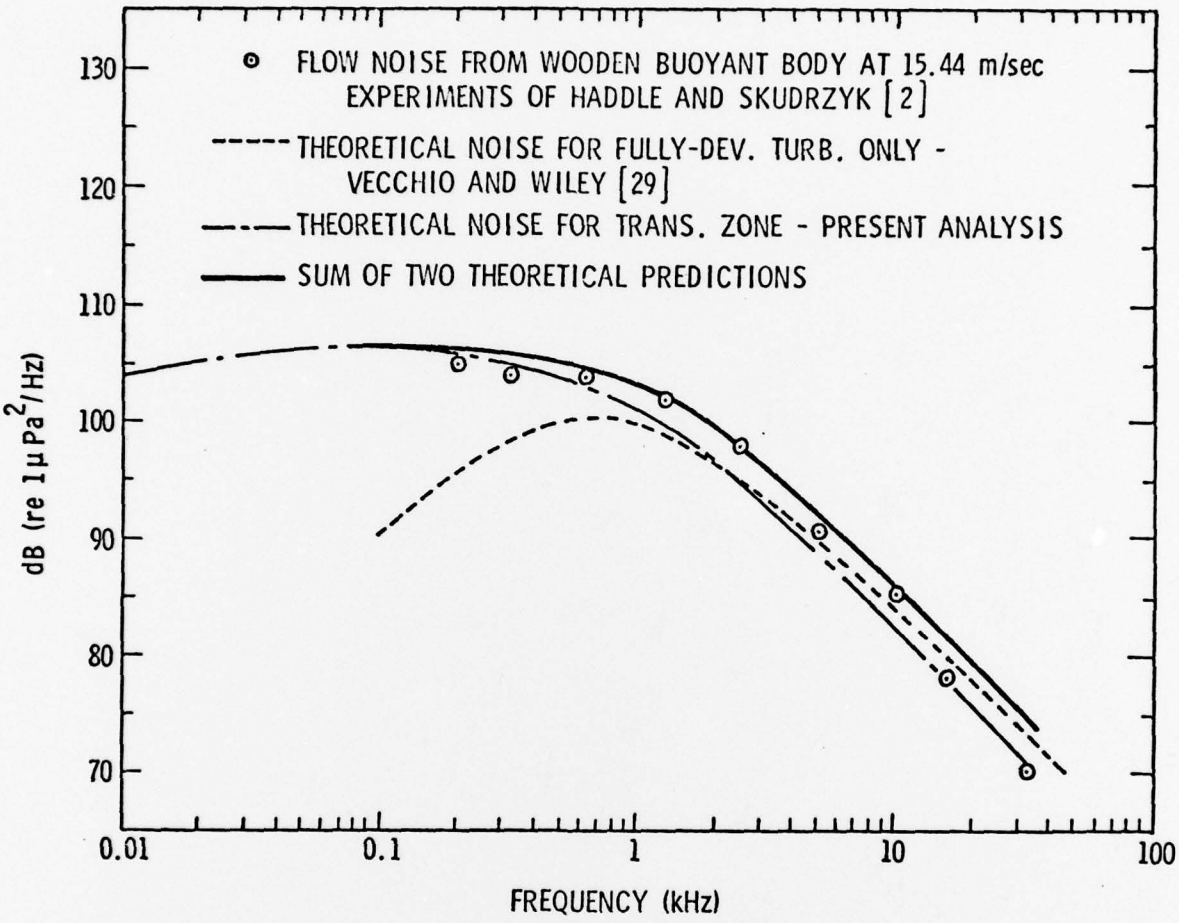

Figure 9. Comparison of the theory with a noise spectrum measured 30 m. away from a buoyantly-propelled wooden vehicle [2].

DISTRIBUTION LIST FOR UNCLASSIFIED TM 78-204 by G. C. Lauchle, dated July 28, 1978

Commander
Naval Sea Systems Command
Department of the Navy
Washington, DC 20362
Attn: Library
Code NSEA-09G32
(Copies No. 1 and 2)

Naval Sea Systems Command
Attn: C. G. McGuigan
Code NSEA-03133
(Copy No. 3)

Naval Sea Systems Command
Attn: L. Benen
Code NSEA-0322
(Copy No. 4)

Naval Sea Systems Command
Attn: E. J. McKinney
Code NSEA-0342
(Copy No. 5)

Naval Sea Systems Command
Attn: E. G. Liszka
Code NSEA-0342
(Copy No. 6)

Naval Sea Systems Command
Attn: G. Sorkin
Code NSEA-035
(Copy No. 7)

Naval Sea Systems Command
Attn: T. E. Peirce
Code NSEA-0351
(Copy No. 8)

Naval Sea Systems Command
Attn: J. G. Juergens
Code NSEA-037
(Copy No. 9)

Naval Sea Systems Command
Attn: H. C. Claybourne
Code NSEA-0371
(Copy No. 10)

Naval Sea Systems Command
Attn: A. R. Paladino
Code NSEA-0372
(Copy No. 11)

Naval Sea Systems Command
Attn: D. Creed
Code NSEA-03132A
(Copy No. 12)

Commander
Naval Ship Engineering Center
Department of the Navy
Washington, DC 20360
Attn: W. L. Louis
Code NSEC-6136B
(Copy No. 13)

Naval Ship Engineering Center
Attn: F. Welling
Code NSEC-6144
(Copy No. 14)

Commanding Officer
Naval Underwater Systems Center
Newport, RI 02840
Attn: C. N. Pryor
Code 01
(Copy No. 15)

Naval Underwater Systems Center
Attn: D. Goodrich
Code 36315
(Copy No. 16)

Naval Underwater Systems Center
Attn: R. J. Kittredge
Code 36313
(Copy No. 17)

Naval Underwater Systems Center
Attn: J. Miguel
Code 36315
(Copy No. 18)

Naval Underwater Systems Center
Attn: B. J. Myers
Code 36311
(Copy No. 19)

Naval Underwater Systems Center
Attn: R. Nadolink
Code 36315
(Copy No. 20)

Naval Underwater Systems Center
Attn: D. A. Quadrini
Code 36314
(Copy No. 21)

DISTRIBUTION LIST FOR UNCLASSIFIED TM 78-204 by G. C. Lauchle, dated July 28, 1978

Naval Underwater Systems Center
Attn: E. J. Sullivan
Code 36311
(Copy No. 22)

Naval Underwater Systems Center
Attn: R. Trainor
Code 36314
(Copy No. 23)

Naval Underwater Systems Center
Attn: F. White
Code 36301
(Copy No. 24)

Naval Underwater Systems Center
Attn: Library
Code 54
(Copy No. 25)

Commanding Officer
Naval Ocean Systems Center
San Diego, CA 92152
Attn: J. W. Hoyt
Code 2501
(Copy No. 26)

Naval Ocean Systems Center
Attn: A. G. Fabula
Code 5311
(Copy No. 27)

Naval Ocean Systems Center
Attn: M. M. Reischman
Code 2542
(Copy No. 28)

Naval Ocean Systems Center
Attn: G. L. Donohue
Code 2542
(Copy No. 29)

Commanding Officer and Director
David W. Taylor Naval Ship R&D Center
Department of the Navy
Bethesda, MD 20084
Attn: S. F. Crump
Code 1505
(Copy No. 30)

David W. Taylor Naval Ship R&D Center
Attn: W. B. Morgan
Code 154
(Copy No. 31)

David W. Taylor Naval Ship R&D Center
Attn: R. Cumming
Code 1544
(Copy No. 32)

David W. Taylor Naval Ship R&D Center
Attn: J. McCarthy
Code 1552
(Copy No. 33)

David W. Taylor Naval Ship R&D Center
Attn: T. Brockett
Code 1544
(Copy No. 34)

David W. Taylor Naval Ship R&D Center
Attn: Y. T. Shen
Code 1524
(Copy No. 35)

David W. Taylor Naval Ship R&D Center
Attn: M. Sevik
Code 19
(Copy No. 36)

David W. Taylor Naval Ship R&D Center
Attn: W. K. Blake
Code 1942
(Copy No. 37)

David W. Taylor Naval Ship R&D Center
Attn: T. M. Farabee
Code 1942
(Copy No. 38)

David W. Taylor Naval Ship R&D Center
Attn: F. C. DeMetz
Code 1942
(Copy No. 39)

David W. Taylor Naval Ship R&D Center
Attn: M. J. Casarella
Code 1942
(Copy No. 40)

DISTRIBUTION LIST FOR UNCLASSIFIED TM 78-204 by G. C. Lauchle, dated July 28, 1978

Commanding Officer and Director
David W. Taylor Naval Ship R&D Center
Department of the Navy
Annapolis Laboratory
Annapolis, MD 21402
Attn: J. G. Stricker
Code 2721
(Copy No. 41)

Commander
Naval Surface Weapon Center
Silver Spring, MD 20910
Attn: G. C. Gaunaurd
Code R-31
(Copy No. 42)

Naval Surface Weapon Center
Attn: Library
(Copy No. 43)

Office of Naval Research
Department of the Navy
800 N. Quincy Street
Arlington, VA 22217
Attn: H. Fitzpatrick
Code 438
(Copy No. 44)

Office of Naval Research
Attn: R. Cooper
Code 438
(Copy No. 45)

Naval Research Laboratory
Washington, DC 20390
Attn: R. J.Hansen
(Copy No. 46)

Defense Documentation Center
5010 Duke Street
Cameron Station
Alexandria, VA 22314
(Copies No. 47 to and including 58)

National Bureau of Standards
Aerodynamics Section
Washington, DC 20234
Attn: P. S. Klebanoff
(Copy No. 59)

Rand Corporation
1700 Main Street
Santa Monica, CA 90406
Attn: R. King
(Copy No. 60)

Rand Corporation
Attn: C. Gazley
(Copy No. 61)

Jet Propulsion Laboratory
Pasadena, CA 01109
Attn: L. Mack
(Copy No. 62)

Hersh Acoustical Engineering
9545 Cozycroft Avenue
Chatsworth, CA 91311
Attn: A. Hersh
(Copy No. 63)

Dynamics Technology, Inc.
3838 Carson Street, Suite 110
Torrance, CA 90503
Attn: W. Haigh
(Copy No. 64)

Dynamics Technology, Inc.
Attn: D. Ko
(Copy No. 65)

Bolt Beranek and Newman
50 Moulton Street
Cambridge, MA 20136
Attn: N. Brown
(Copy No. 66)

Bolt Beranek and Newman
Attn: D. Chase
(Copy No. 67)

Bolt Beranek and Newman
Attn: K. L. Chandiraman
(Copy No. 68)

Massachusetts Institute of Technology
77 Massachusetts Avenue
Cambridge, MA 02139
Attn: Prof. Patrick Leehey
Dept. of Ocean Engineering
Room 5-222
(Copy No. 69)

DISTRIBUTION LIST FOR UNCLASSIFIED TM 78-204 by G. C. Lauchle, dated July 28, 1978

Dr. J. L. Lumley
Sibley School of Mechanical and
Aeronautical Engineering
Upson Hall
Cornell University
Ithaca, NY 14850
(Copy No. 70)

Dr. D. G. Crighton
University of Leeds
Department of Applied Mathematical Studies
Leeds LS29JT
England
(Copy No. 71)

Applied Research Laboratory
The Pennsylvania State University
Post Office Box 30
State College, PA 16801
Attn: B. R. Parkin
(Copy No. 72)

Applied Research Laboratory
Attn: E. J. Skudrzyk
(Copy No. 73)

Applied Research Laboratory
Attn: G. H. Hoffman
(Copy No. 74)

Applied Research Laboratory
Attn: F. H. Fenlon
(Copy No. 75)

Applied Research Laboratory
Attn: G. C. Lauchle
(Copy No. 76)

Applied Research Laboratory
Garfield Thomas Water Tunnel File
(Copy No. 77)